Available online at https://link.springer.com/journal/42241
http://www.jhydrodynamics.com
Journal of Hydrodynamics, 2020, 32(6): 1071-1079
https://doi.org/10.1007/s42241-020-0071-8

Numerical simulations of propeller cavitation flows based on OpenFOAM *

Min-sheng Zhao, Wei-wen Zhao, De-cheng Wan
Computational Marine Hydrodynamics Lab (CMHL), State Key Laboratory of Ocean Engineering, School of Naval Architecture, Ocean and Civil Engineering, Shanghai Jiao Tong University, Shanghai 200240, China

(Received October 9, 2020, Revised October 22, 2020, Accepted October 23, 2020, Published online November 26, 2020)
©China Ship Scientific Research Center 2020

Abstract: In order to study the cavitation and hydrodynamic characteristics of propeller under uniform and non-uniform flows, numerical investigations are performed using interPhaseChangeDyMFoam in the open source computational fluid dynamics (CFD) software platform OpenFOAM with Schnerr-Sauer cavitation model. The simulation results can be used as a reference to evaluate the working ability of a propeller in case of actual navigation. A new grid encryption method is adopted in the research to better capture the existence of vortex cavitation at the propeller tip. The method of function input is carried out in the study to simulate the condition of non-uniform flow and reduce the calculation amount. Typical unsteady dynamics are predicted by the Reynolds-averaged Navier-Stokes (RANS) method with a modified shear stress transport (SST) k-ω turbulence model. The numerical results of the propeller such as cavitation shape and pressure distribution under uniform and non-uniform flow are analyzed and compared with each other.

Key words: OpenFOAM, E779A propeller, cavitation, non uniform flow

Introduction

The study of cavitation plays an important role in today's hydrodynamics research. Such phenomenon contains many complex flows known in hydrodynamics, including turbulence, two-phase flow and so on. Up to now, there are still some limitations in people's understanding about the formation mechanism of cavitation and the dynamics involved in the shedding of the cavitation period. With the development of industry, hydrodynamic equipment always operates at high speed condition, which makes it difficult to avoid cavitation, and the vibration and noise caused by the phenomenon affect the hydrodynamic performance of equipment. Therefore, the research on the unsteady characteristics of cavitation has always been a hot topic of fluid mechanics.

* Project supported by the National Natural Science Foundation of China (Grant Nos. 51879159, 51809169 and 51909160), the National Key Research and Development Program of China (Grant Nos. 2019YFB1704200, 2019YFC0312400), the Chang Jiang Scholars Program (Grant No. T2014099) and the Innovative Special Project of Numerical Tank of Ministry of Industry and Information Technology of China (Grant No. 2016-23/09).
Biography: Min-sheng Zhao (1994-), Male, Ph. D. Candidate,
E-mail: zhaominsheng@sjtu.edu.cn
Corresponding author: De-cheng Wan,
E-mail: dcwan@sjtu.edu.cn

Researchers have done a lot of experiments on cavitation in the laboratory, these data and observed phenomena are of great help to study the mechanism and characteristics of cavitation. Cavitation can be generally categorized as sheet cavitation, cloud cavitation and super cavitation. Katz[1] studied the formation process of cavitation, and the relation between cavitation shape and mixing-layer eddy structure using holographic and schlieren flow display of supercavitation around hydrofoil show the characteristics of supercavitation distribution and pressure oscillation. Duttweiler and Brennen[2] experimentally studied the problems of the surge instability of a cavitating propeller.

With the development of the research, the shortcomings of the experimental methods have gradually emerged. The experimental results have unbreakable technical constraints, such as scale effect. In addition, it is very expensive and time-consuming to carry out experimental research on the cavitation structure of a real marine propeller. Therefore the numerical simulation of cavitation has become a trend. The computational fluid dynamics (CFD) results obtained by Ji et al.[3] verify the connection between the pressure fluctuations and the changing cavitation patterns as the blades sweep through the high velocity wake region. Zhang et al.[4] studied the effect of obstacles on the surface of hydrofoil on cavitation. The experimental and numerical results show that

small-scale cavitation shedding is the dominant factor of cavitation flow.

Wang et al.[5] used Saito cavitation model and shear stress transport-scale adaptive simulation (SST-SAS) turbulence model to study the cavity evolution process and cavitation induced pressure signals. The predicted results are rather satisfying, especially the cavity collapse induced shock wave emission and its interaction with the attached cavity sheet. The unsteady cavitation patterns and their evolution around a Delft twisted hydrofoil were simulated by Ji et al.[6], and the numerical results indicate that the cavity volume fluctuates drastically as the cavitating flow develops with cavity growth, destabilization, and collapse. Liang et al.[7] carried out the numerical simulation of cavitation around hydrofoil based on adaptive mesh refinement. Wang et al.[8] applied a dynamic cubic nonlinear sub-grid scale model to simulate the unsteady cavitating flow around a 3-D Clark-Y hydrofoil. Peng et al.[9] investigated the effects of both flow field and water qualities on tip vortex cavitation inception with experiments and numerical simulations considered. Simulations of cavitating flows are successfully achieved to precisely characterize the features of cavitation with automa tically and dynamically refining the mesh by Li et al.[10].

The analysis of the dynamic mechanism involved in the cavitation process has also attracted the attention of researchers. Scholars use different cavitation models to carry out numerical research and improve the cavitation model. Maiga et al.[11] applied the multibubble model of the modified Rayleigh-Plesset equation to the research of interactions between bubbles' primary importance in the first moments of the cavitation development. Karabelas and Markatos[12] investigated the condensation of water-vapor in the convective flow on airfoil geometry, with the turbulence influence accounted by Spalart-Allmaras one-equation model. The transport equation model (TEM) with a governing equation for the liquid-vapor phase fraction has been used. Rodi[13] compared the numerical results of the LES method and Reynolds-averaged Navier-Stokes (RANS) method for the cavitation flow around the bluff bodies with experimental approach. Yang et al.[14] simulated the cavitating flows in a Francis turbine operating under the overload conditions by using the Zwart-Gerber-Belamri (ZGB) cavitation model. Liu et al.[15] studied the difference among-different cavitation models in the simulation of hydrofoil cavitating flow.

Based on the evaluations of existing models, Huang and Wang[16] identified the differences in the affected region between two vaporization and condensation processes, and provided a modified density based cavitation model. Passandideh-Fard et al.[17] simulated the cavitating flows around Clark-Y hydrofoil using LES method and volume of fluid (VOF) technique. The turbulent attached cavitating flow around a Clark-Y hydrofoil is investigated by the large eddy simulation (LES) method coupled with a homogeneous cavitation model by Ji et al.[18]. Cheng et al.[19] proposed a coupled Euler-Lagrangian cavitation model considering the gas core effect, which significantly improved the prediction accuracy of tip gap vortex cavitation.

The hydrodynamic performance and cavitation characteristics of the propeller have also been studied[20]. Potential flow method is a commonly used numerical method in propeller performance analysis, Kinnas et al.[21] have made outstanding achievements in this field. Viscous flow CFD method does not need artificial treatment of Kutta conditions, and has developed rapidly in recent years. The cavitating flow of highly skewed propeller in uniform flow and wake is simulated by Ji et al.[22]. Compared with the experimental results, it can be seen that the thrust coefficient and torque coefficient of the propeller have been predicted satisfactorily. The unsteady viscous marine propellers are calculated by sliding grid function and the results are compared with the measured data by Funeno[23].

At present, domestic scholars mainly study the characteristics of propeller cavitation flow based on commercial software[24]. Although their simulation results are satisfactory and in good agreement with experiments, the disadvantage of using commercial software is that we are limited in our own research and development. Therefore, in the present work, all the simulation calculations of open water characteristics of propeller are obtained using interPhaseChangeDyMFoam in the open source CFD software platform OpenFOAM with Schnerr-Sauer cavitation model. In order to reduce the calculation cost, a new grid encryption method is adopted in the research. The numerical results in open water of E779A propeller are compared with experimental data. The unsteady characteristics of the sheet and tip cavitation on the propeller surface have been studied.

1. Numerical method

1.1 *Governing equations*

According to the assumption of single-phase homogeneity in Schnerr-Sauer cavitation model, the mixed medium composed of vapor and liquid is replaced by a single-phase whose density varies with pressure. Meanwhile, the mass exchange process between vapor and liquid is described based on the transport equation. The continuity equation (1) and momentum equation (2) can be obtained.

$$\frac{\partial \rho}{\partial t}+\nabla \cdot(\rho U)=0 \tag{1}$$

$$\frac{\partial}{\partial t}(\rho U)+\nabla \cdot(\rho U U)=\nabla p+\frac{\partial \rho}{\partial t}+\nabla \cdot \mu \nabla U+\rho g+F \tag{2}$$

In the above equations, ρ and μ represent density and viscosity coefficient. The density and viscosity coefficient of mixed homogeneity are determined by the following equation:

$$\rho_m=\rho_l \alpha_l+\rho_v(1-\alpha_l) \tag{3}$$

$$\mu_m=\mu_l \alpha_l+\mu_v(1-\alpha_l) \tag{4}$$

In the above equations, the subscript v and l represent the gas phase and liquid phase respectively, and the subscript m represents the mixed medium, α_l is the volume fraction of liquid phase.

1.2 *Mass transfer model*

Schnerr Sauer cavitation model is a model based on transport equation, which uses different source terms to represent condensation and vaporization process to simulate mass transfer between gas and liquid. It is derived from Rayleigh Plesset equation, which read as follows:

$$\frac{\left|P_v-P\right|}{\rho_L}=\frac{3}{2}\left(\frac{\mathrm{d}R}{\mathrm{d}t}\right)^2+R\frac{\mathrm{d}^2R}{\mathrm{d}t^2}+\frac{1}{\rho_L}\left(4\gamma_L\frac{\mathrm{d}R}{\mathrm{d}t}+2\frac{\sigma}{R}\right) \tag{5}$$

$$\frac{\mathrm{D}R}{\mathrm{D}t}=\sqrt{\frac{2}{3}\frac{P_B-P}{\rho_l}} \tag{6}$$

When the R-P equation is used, the viscous force term and the surface tension term are generally ignored. At the same time, the second derivative term in the schnerr Sauer model is also ignored. Then the formula is obtained and the approximate wall expansion velocity is derived.

The volume fraction of the gas phase in the Schner-Sauer cavitation model is also related to the density and radius of the gas core. The expression of mass source term for condensation rate and vaporization rate are as follows:

$$\dot{m}_c=C_c\frac{3\rho_v\rho_l\partial_v(1-\alpha_v)}{\rho R},\ \ \mathrm{sgn}(P_v-P)\sqrt{\frac{2\left|P_v-P\right|}{3\rho_l}} \tag{7}$$

$$\dot{m}_v=-C_v\frac{3\rho_v\rho_l\partial_v(1-\alpha_v)}{\rho R},\ \ \mathrm{sgn}(P_v-P)\sqrt{\frac{2\left|P_v-P\right|}{3\rho_l}} \tag{8}$$

The radius of gas core R meets the following equation

$$\alpha_v=\frac{n_0\frac{4}{3}\pi R^3}{n_0\frac{4}{3}\pi R^3+1} \tag{9}$$

1.3 *Turbulence model*

In this paper, the SST $k\text{-}\Omega$ model proposed by Mender is used to simulate the Reynolds stress. This model is a combination of $k\text{-}\Omega$ model and $k\text{-}\varepsilon$ model. The former is used in the far field, and the latter is used near the wall. This is because the denominator near the wall in the expression of $k\text{-}\varepsilon$ model tends to close to zero, resulting in divergence. The main equations of the model are as follows:

$$\frac{\partial \rho k}{\partial t}+\frac{\partial \rho u_i k}{\partial x_i}=P_k-\beta^*\rho k\omega+\frac{\partial}{\partial x_i}\left[(\mu+\sigma_k\mu_t)\frac{\partial k}{\partial x_i}\right] \tag{10}$$

$$\alpha\rho S^2P_k-\beta\rho\omega^2+\frac{\partial}{\partial x_i}\left[(\mu+\sigma_\omega\mu_t)\frac{\partial \omega}{\partial x_i}\right]+2(1-F_1)\rho\sigma_{\omega 2}\frac{1}{\omega}\frac{\partial k}{\partial x_i}\frac{\partial \omega}{\partial x_i}=\frac{\partial \rho\omega}{\partial t}+\frac{\partial \rho u_i\omega}{\partial x_i} \tag{11}$$

where F_1 is the harmonic equation of the model, when the value approaches 1, it is expressed as $k\text{-}\Omega$ model, when the value approaches 0, it is expressed as $k\text{-}\varepsilon$ model.

Considering the influence of turbulence viscosity on cavitation process simulation, Rebound et al.[25] proposed adding an artificial term to reduce the viscosity and better predict the cavitation frequency. The modified equation is as follows:

$$\mu_t=f(\rho)C_\omega\frac{k}{\omega} \tag{12}$$

$$f(\rho)=\rho_v+\frac{(\rho_m-\rho_v)^n}{(\rho_l-\rho_v)^{n-1}},\ \ n\gg 1 \tag{13}$$

1.4 *Simulation setup*

The E779A propeller is used as the research

object for the numerical simulation of the cavitation characteristics of the propeller. This propeller has rich test data and the basis of numerical simulation research in different fields. It is also one of the two commonly used propellers in the world in the cavitation research, along with the PPTC propeller. The E779A propeller is a symmetrical four blade propeller. The parameters such as disc surface ratio and pitch ratio are shown in Table 1.

Table 1 E779A propeller parameters

Items	Value
Diameter, D	0.253
Rotor diameter, d/D	0.200
Nacelle diameter, $P_{0.7}/D$	1.100
Height of tower, A_e/A_o	0.689

This research is based on the two-phase flow solver interPhaseChangeDyMFoam in OpenFOAM, which is an open-source CFD operating platform. In the realization of propeller rotation, it is not necessary to use the rotation coordinate reference system of relative motion for calculation. This method is only suitable for steady simulation, and the advantage is to study a single blade, which can reduce the calculation cost. Instead, this study directly uses the sliding grid technology to simulate the actual flow of the propeller under the condition of the rotation of the flow. In order to make a good compatibility effect of mesh in rotation, the cylindrical calculation domain is generally constructed, and the internal is the slip region. The overall calculation domain layout, internal slip surface and propeller surface grid layout are shown in Figs. 1 and 2.

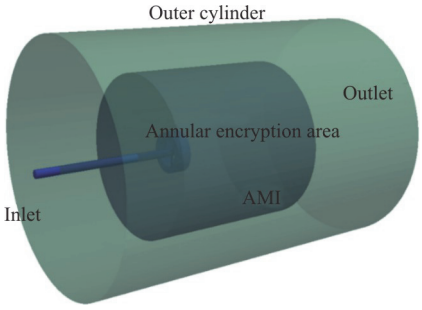

Fig. 1 (Color online) Computational domain and slip surface layout

Through the study in advance, the grid layout method is optimized, that is to add an annular encryption area around the tip of propeller blade, as shown in Fig. 3. This annular encrypted region is selected to encircle the edge of the propeller disk, which is exactly where the tip vortices appear. In this way, the area of the encrypted region can be reduced,

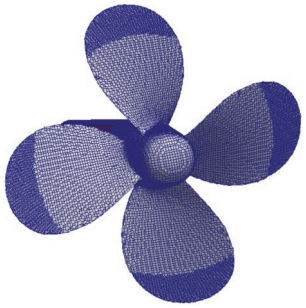

Fig. 2 (Color online) Propeller surface mesh distribution

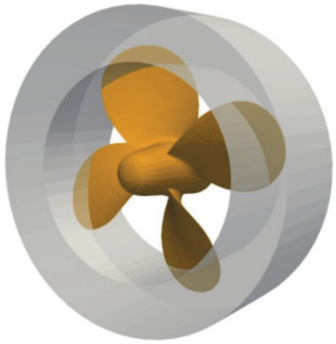

Fig. 3 (Color online) Annular encrypted region

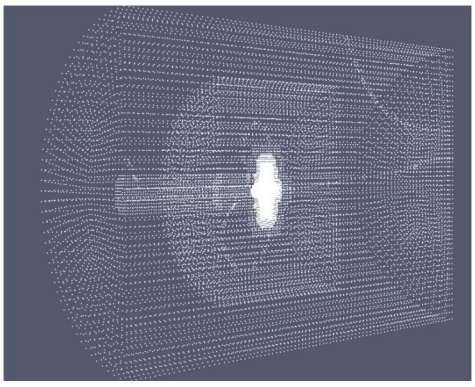

Fig. 4 Coarse grid layout

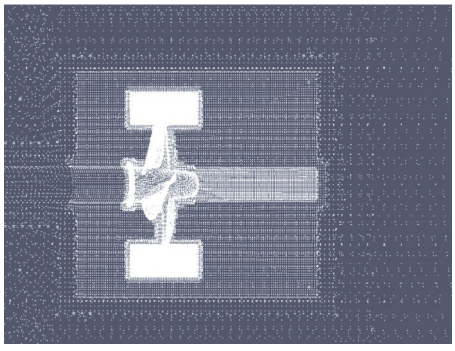

Fig. 5 Mesh distribution in mid-plane with annular encrypted region

that is to say, the amount of mesh can be reduced and the accuracy of capturing the tip vortex cavitation can be improved all at time. Meanwhile, an encrypted area is added at the back of the propeller hub to capture the hub vortex cavitation. Figures 4 and 5 show the grid distribution in the general grid layout strategy by using the sketch map of grid points with two mesh generation methods. There is a three-level dense area around the propeller, and the grid is densified on the blade surface. In order to ensure enough calculation accuracy and improve calculation efficiency as much as possible, the total amount of grid is about 5×10^6.

2. Results and discussion

2.1 *The results of open-water characteristics*

Firstly, the open water performance of E779A propeller is simulated to verify the effectiveness of the numerical method and lay a good foundation for cavitation flow simulation. Under the open water condition, the speed of the propeller is stable at about 25 r/s, and the advance coefficients are 0.40, 0.60, 0.71 and 0.83 respectively, all of which are normal forward flow. See Table 2 for the calculated propeller thrust coefficient.

From the data in Table 2, it can be seen that the thrust coefficient calculated under uniform flow is close to the experimental value as a whole, and the error is small when the advance coefficient is low; when the advance coefficient is increased, the error increases slightly to about 5%. The simulation results of propeller's open water performance are good with reliability and accuracy.

Table 2 Open water characteristics simulation

J	K_T (exp.)	K_T (num.)	Error
0.60	0.293	0.281	4.09%
0.71	0.247	0.234	5.26%
0.77	0.215	0.202	6.04%
0.83	0.170	0.159	6.47%

2.2 *Simulation on E779A propeller in cavitation flow*

According to the propeller speed and cavitation number in the literature, the far-field pressure value set in OpenFOAM is calculated. The formula is as follows, and the parameters in cavitation simulation are also listed in Table 3

$$\sigma_n = \frac{p - p_v}{0.5\rho(nD)^2} \tag{14}$$

Firstly, the cavitation characteristics of the propeller are simulated under the coarse grid, as shown in Fig. 6. And it can be seen that the tip part of the blade captures the existence of the tip vortex cavitation well, and the shape and size are stable. The generation and development of hub vortex cavitation are also well simulated. Because of the low mesh size and the density of mesh at the tip vortex position, the length of the cavity captured is limited, which is also to save calculation.

Table 3 Simulation parameter setting

Parameter	Value
Rotating speed/r·s^{-1}	24.97
Advance coefficients	0.77
Cavitation number	1.783
Saturated vapor pressure/Pa	2818
Kinematic viscosity/m^2·s^{-1}	9.34×10^{-7}
Density of water/kg·m^{-3}	997.44

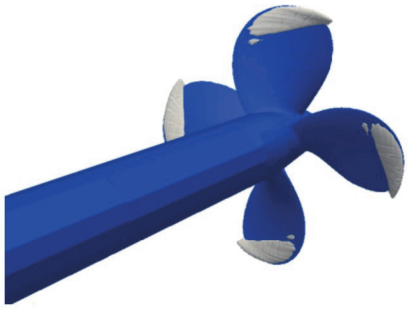

(a) Cavitation distribution on suction surface of propeller

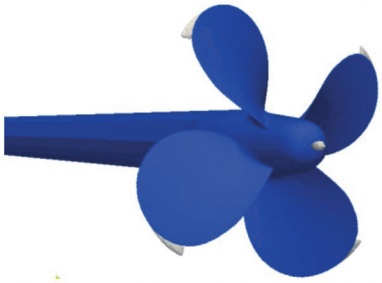

(b) Tip vortex cavitation and hub vortex cavitation

Fig. 6 (Color online) Cavitation simulation with coarse grid

Figures 7 and 8 show the propeller cavitation pattern after the annular shape of the tip vortex is encrypted. It is obvious that the length of the tip vortex cavitation captured in the simulation has increased. The cavitation of the propeller is mainly formed on the suction surface of the propeller and falls off from the tip of the blade. In terms of the effect, the method of turbulence model, cavitation model and grid division is very effective to capture the cavitation of the propeller tip. In order to show that the numerical simulation of cavitation flow of propeller depends on the detailed grid, we put the tip vortex cavitation calculated by numerical calculation together with the densified area of propeller tube in Fig. 4, and we can see that the tip vortex cavitation that can be captured is the tip vortex that appears in the encrypted area of the tube. Theoretically, as long

as the tube area used for encryption is long enough, the captured tip vortex cavitation can be long enough. However, this method will increase the computational cost.

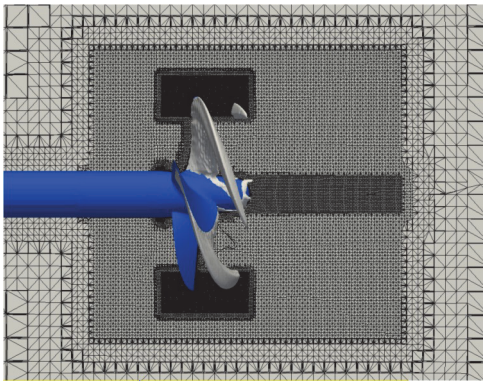

Fig. 7 (Color online) Mesh and cavitation distribution in mid-plane

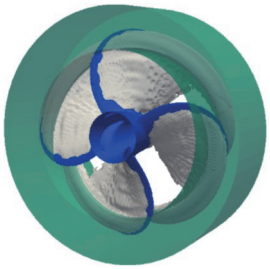

Fig. 8 (Color online) Tip vortex cavitation in refined tube

In addition, some researchers have proposed a method to encrypt only the trajectory region of tip vortex cavitation. In theory, this method can save more calculation and improve the efficiency of numerical simulation. However, due to the need of the approximate range of the tip vortex cavitation, the applicability of different calculation examples is low.

The following figures show the cavitation process of E779A impeller under uniform inflow condition. First of all, it can be seen that the blade cavitation initially occurs on the suction surface of the blade back, and then the tip vortex cavitation appears and develops outward along the blade tip. In the process of the tip vortex cavitation extending backward, the cavity maintains a stable and regular shape, and the volume of the bubble does not change much in the x-axis direction. The length range of tip vortex cavitation is basically consistent with that of the annular dense region around the propeller mentioned above. It can be seen that with the development of cavitation, the hub vortex cavitation also appears at the propeller hub. However, the shape of the hub vortex cavitation is irregular. As shown in Fig. 9, it is relatively scattered cavitation and does not extend backward along the dense area.

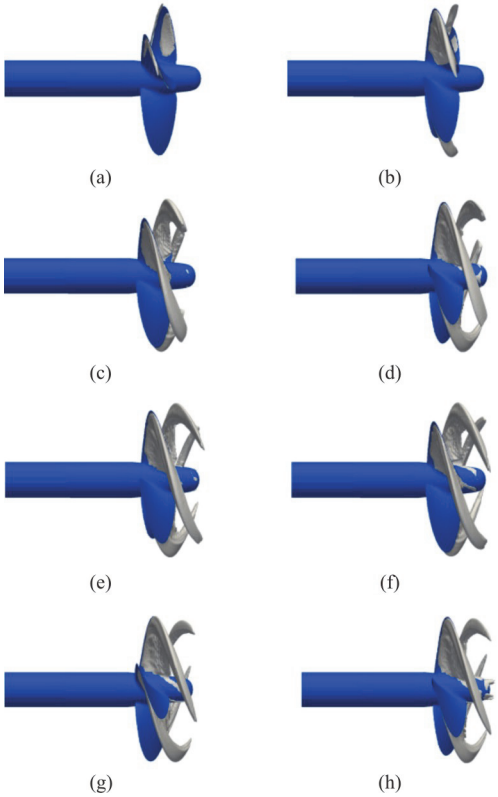

Fig. 9 (Color online) Cavitation shape development under uniform inflow

Figure 10 shows the cavitation and change cloud picture of propeller under the condition of non-uniform inflow. It can be seen that the shape of tip vortex cavitation has become irregular in the backward development process, and it does not extend backward along the helix like the bubble in uniform flow. The volume of cavitation in the x-axis direction has an obvious increase, and the position of the cavitation in the positive direction of z-axis, but this trend is not obvious, the propeller hub position produces obvious hub vortex cavitation, at this time, the hub vortex cavitation is also not a circular cylinder, but dispersed backward, there is a hollow area in the middle, the overall backward development.

The distance is obviously longer than that under uniform flow condition, so the reason why the cavitation of hub vortex is not fully developed should not be the grid factor. On the whole, the tip vortex and hub vortex cavitation produced by propeller under non-uniform flow condition have larger volume and more irregular shape than those under uniform flow condition. The backward development distance in the x-axis direction is longer and the non-uniformity is obvious.

Liu[26] proposed a new cavitation model, which is an improvement on the original transport equation

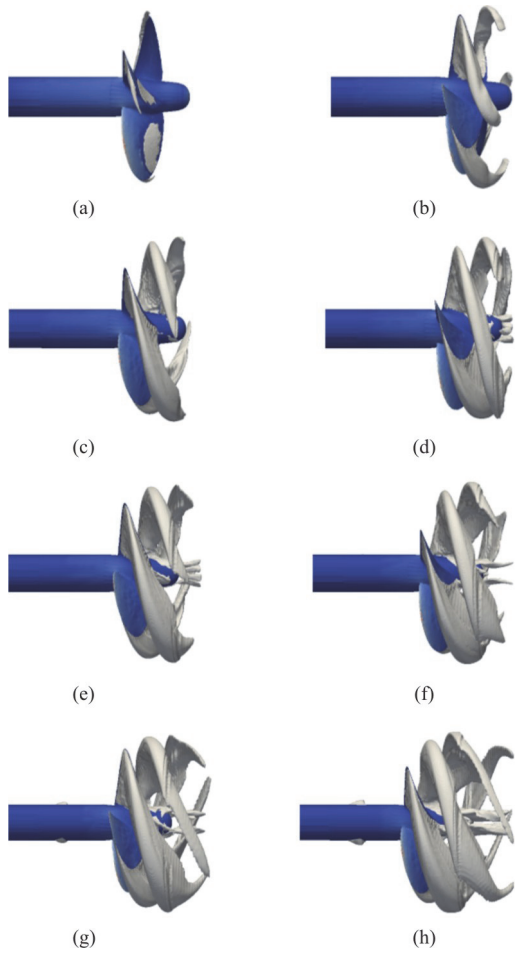

Fig. 10 (Color online) Cavitation shape development under non-uniform inflow

model with the second derivative term reserved. When the original bubble model is derived from the R-P equation, the second derivative of the average bubble radius is usually ignored. Liu's idea is to retain this physical quantity and then carry out derivation and numerical simulation. Figure 11 shows the experimental observation chart obtained by Francesco et al.[27], the simulation results of Liu's calculation and the simulation diagram of this study. Obviously, better simulation results can be obtained when the second-order small quantities are ignored. The results show that the developed tip vortices can be captured well, and the blade cavitation along the suction surface of propeller blade can also be well simulated.

2.3 *Pressure distribution*

The thrust of the propeller comes from the pressure difference between the suction surface and the back of the blade. When the incoming flow reaches the leading edge of the blade, a low-pressure area is formed on the suction side under the action of flow separation. However, according to the mechanism of cavitation, when the pressure in the low-pressure area

Fig. 11 (Color online) Overset grid arrangement

of the suction side drops to the saturated vapor pressure of the liquid at this temperature, cavitation will occur locally, and the pressure in the cavitation area will no longer drop. Figure 12 shows the comparison of the pressure distribution on the suction surface of the propeller under three different conditions. Under the same pressure scale, it is obvious that the colors are different, which means the pressure on the blade surface is different. When cavitation occurs, the suction surface pressure of the blade is significantly higher, which is consistent with the previous research results[28].

When the air mass flows from the suction surface away from the side of the leading edge, due to the existence of the high pressure area, it will gradually collapse and liquefy, and the pressure will return to be consistent with the surrounding flow field. That is to say, the region of cavitation will restrain the formation

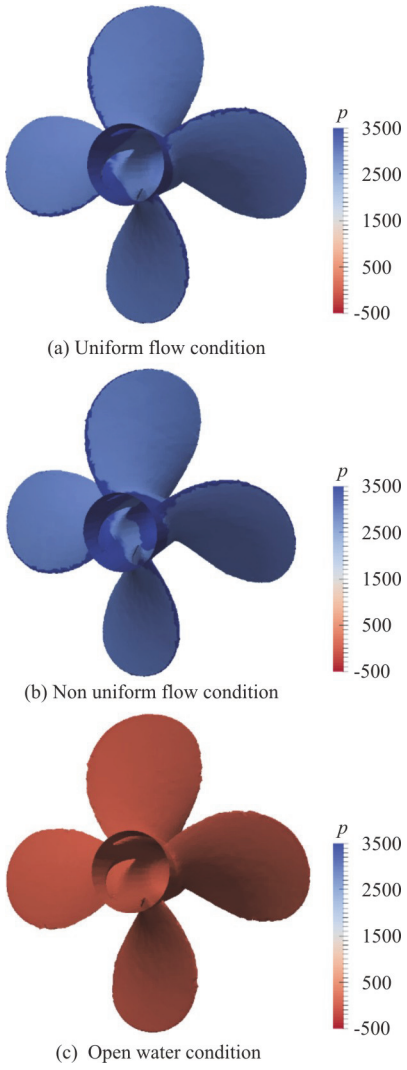

Fig. 12 (Color online) Pressure distribution on suction surface

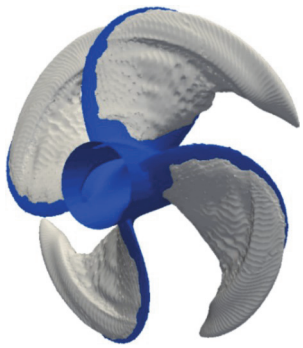

Fig. 13 (Color online) Cavitation distribution on suction surface

of low pressure region. It can also be seen from Fig. 13 that cavitation occurs in areas where the pressure decreases relatively more. The simulation results are consistent with those of Chen's calculation and analysis of the cavitation flow of PPTC propeller, which also verifies the reliability of the simulation method.

This kind of restraining effect makes the pressure difference between two sides of the blade lower, and then reduces the propeller thrust. From Figs. 12(a) and 12(b) it can be seen that the pressure distribution on the suction surface of the propeller blade is not significantly different under the conditions of uniform flow and non-uniform flow, and the non-uniform flow does not significantly affect the pressure distribution on the blade surface. Figures 14 and 15 show the average pressure and average velocity at 0.5 and 2.0 times radius distance behind the propeller, which shows the influence of propeller on wake.

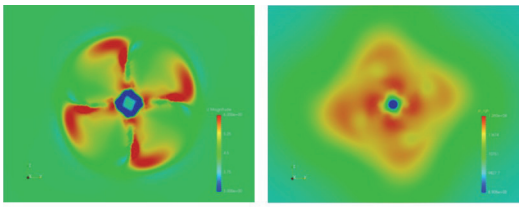

Fig. 14 (Color online) Wake field at $0.5R$

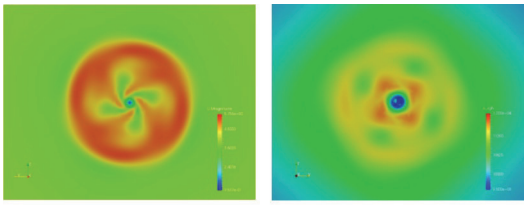

Fig. 15 (Color online) Wake field at $2.0R$

3. Conclusions and prospect

Based on the open-source CFD platform OpenFOAM, the dynamic grid two-phase flow solver interPhaseChangeDyMFoam is used to simulate the cavitation and hydrodynamic performance of the propeller. Compared with the experimental results of open water with uniform flow, the numerical method has certain reliability. The method applied in the preset work to simulate propeller cavitation flow is also feasible. It can be seen from the cavitation simulation results of the propeller that:

(1) The numerical method based on the sliding grid and the transport equation model can simulate the tip and hub vortices of propeller very well. The existence of tip vortex cavitation can be better captured by ring grid encryption of blade tip, which has higher universality and can improve the calculation efficiency.

(2) Using function input method to simulate non-uniform flow can improve the computational efficiency and obtain satisfactory simulation results. Under the condition of non-uniform flow, the tip

vortex cavitation volume increases and extends to the rear of the propeller shaft, and the hub vortex cavitation is obvious. However, the influence of this condition on the suction surface pressure distribution is not significant.

(3) Further research shows that the cavitation will hinder the pressure drop on one side of the suction surface of the propeller, reduce the pressure difference on both sides of the blade, and then reduce the thrust coefficient.

(4) The function input used in this paper can simulate the unsteady cavitation of propeller with less calculation. The later research will focus on the extraction and application of the flow field information of the stern wake, and better simulate and study the propeller cavitation based on the actual flow.

References

[1] Katz J. Cavitation phenomena within regions of flow separation [J]. *Journal of Fluid Mechanics*, 2006, 140: 397-436.

[2] Duttweiler M. E., Brennen C. E. Surge instability on a cavitating propeller [J]. *Journal of Fluid Mechanics*, 2001, 458: 133-152.

[3] Ji B., Luo X., Peng X. et al. Numerical analysis of cavitation evolution and excited pressure fluctuation around a propeller in non-uniform wake [J]. *International Journal of Multiphase Flow*, 2012, 43: 13-21.

[4] Zhang L. X., Chen M., Deng J. et al. Experimental and numerical studies on the cavitation over flat hydrofoils with and without obstacle [J]. *Journal of Hydrodynamics*, 2019, 31(4): 708-716.

[5] Wang C. C., Hunag B., Wang G. Y. et al. Numerical simulation of transient turbulent cavitating flows with special emphasis on shock wave dynamics considering the water/vapor compressibility [J]. *Journal of Hydrodynamics*, 2018, 30(4): 573-591.

[6] Ji B., Luo X., Wu Y. et al. Numerical analysis of unsteady cavitating turbulent flow and shedding horse-shoe vortex structure around a twisted hydrofoil [J]. *International Journal of Multiphase Flow*, 2013, 51: 33-43.

[7] Liang S., Li Y., Wan D. C. Numerical simulation of cavitation around Clark-Y hydrofoil based on adaptive mesh refinement [J]. *Chinese Journal of Hydrodynamics*, 2020, 35(1): 1-8(in Chinese).

[8] Wang Z. Y., Huang X. Y., Cheng H. Y. et al. Some notes on numerical simulation of the turbulent cavitating flow with a dynamic cubic nonlinear sub-grid scale model in OpenFOAM [J]. *Journal of Hydrodynamics*, 2020, 32(4): 790-794.

[9] Peng X. X., Zhang L. X., Wang B. L. et al. Study of tip vortex cavitation inception and vortex singing [J]. *Journal of Hydrodynamics*, 2019, 31(6): 1170-1177.

[10] Li L. M., Hu D. Q., Liu Y. C. et al. Large eddy simulation of cavitating flows with dynamic adaptive mesh refinement using OpenFOAM [J]. *Journal of Hydrodynamics*, 2020, 32(2): 398-409.

[11] Maiga M. A., Coutier-Delgosha O., Buisine D. Cavitation in a hydraulic system: The influence of the distributor geometry on cavitation inception and study of the interactions between bubbles [J]. *International Journal of Engine Research*, 2016, 17(5): 543-555.

[12] Karabelas S. J., Markatos N. C. Water vapor condensation in forced convection flow over an airfoil [J]. *Aerospace Science and Technology*, 2008, 12(2): 150-158.

[13] Rodi W. Comparison of LES and RANS calculations of the flow around bluff bodies [J]. *Journal of Wind Engineering and Industrial Aerodynamics*, 1997, 69-71: 55-75.

[14] Yang J., Zhou L. J., Wang Zheng-wei et al. Numerical investigation of the cavitation dynamic parameters in a Francis turbine draft tube with columnar vortex rope [J]. *Journal of Hydrodynamics*, 2019, 31(5): 931-939.

[15] Liu Y., Wang J., Wan D. Numerical simulations of cavitation flows around Clark-Y hydrofoil [J]. *Journal of Applied Mathematics and Physics*, 2019, 7(8): 1660-1676.

[16] Huang B., Wang G. Y. A modified density based cavitation model for time dependent turbulent cavitating flow computations [J]. *Chinese Science Bulletin*, 2011, 56(19): 1985-1992.

[17] Passandideh-Fard M., Zahiri A. P., Roohi E. Numerical simulation of cavitation around a two-dimensional hydrofoil using VOF method and LES turbulence modelm [J]. *Applied mathematical modelling*, 2013, 37(9): 6469-648.

[18] Ji B., Long Y., Long X. P. et al. Large eddy simulation of turbulent attached cavitating flow with special emphasis on large scale structures of the hydrofoil wake and turbulence-cavitation interactions [J]. *Journal of Hydrodynamics*, 2017, 29(1): 27-39.

[19] Cheng H., Long X., Ji B. et al. A new Euler-Lagrangian cavitation model for tip-vortex cavitation with the effect of non-condensable gas [J]. *International Journal of Multiphase Flow*, 2021, 134: 103441.

[20] Hou L., Hu A. Theoretical investigation about the hydrodynamic performance of propeller in oblique flow [J]. *International Journal of Naval Architecture and Ocean Engineering*, 2019, 11(1):119-130.

[21] Kinnas S., Hsin C. Y., Keenan D. A. Potential based panel method for the unsteady flow around open and ducted propellers [C]. *Proceedings of the 8th Symposium on Naval Hydrodynamics*, Ann Arbor, Michigan, USA, 1990.

[22] Ji B., Luo X., Wang X. et al. Unsteady numerical simulation of cavitating turbulent flow around a highly skewed model marine propeller [J]. *Journal of Fluids Engineering*, 2011,133(1): 011102.

[23] Funeno I. Analysis of unsteady viscous flows around a highly skewed propeller [J]. *Journal of the Kansai Society of Naval Architects*, *Japan*, 2002, 237: 39-45.

[24] Cai R. Q., Cheng F. M., Feng X. M. Calculation and analysis of the open water performance of propeller by CFD software Fluent [J]. *Journal of Ship Mechanics*, 2006, 10(5): 41-48.

[25] Reboud J. L., Stutz B., Coutier-Delgosha O. Two phase flow structure of cavitation experiment and modeling of unsteady effects [C]. *Proceedings of the 3rd International Symposium on Cavitation*, Grenoble, France, 1998.

[26] Liu D. The numerical simulation of propeller sheet cavitation with a new cavitation model [J]. *Procedia Engineering*, 2015, 126: 310-314.

[27] Francesco S., Claudio T., Luca G. A viscous/inviscid coupled formulation for unsteady sheet cavitation modeling of marine propeller [C]. *Fifth International Symposium on Cavitation*, Osaka, Japan, 2003.

[28] Zhao M., Wan D. C., Chen G. Comparison of SST k-ω and Smagorinsky model in cavitation simulation around NACA0012 [C]. *Proceedings of the Twenty-Ninth International Ocean and Polar Engineering Conference*, Honolulu, Hawaii, USA, 2019.